Title
Up-regulation of Wnt/β-catenin expression is accompanied with vascular repair after traumatic brain injury

Journal
Cerebrovascular and Brain Metabolism Reviews, 38(2)

ISSN
1040-8827

Authors
Salehi, Arjang
Jullienne, Amandine
Baghchechi, Mohsen
et al.

Publication Date
2018-02-01

DOI
10.1177/0271678x17744124

Peer reviewed

Original Article

JCBFM

Journal of Cerebral Blood Flow & Metabolism
2018, Vol. 38(2) 274–289

DOI: 10.1177/0271678X17744124
journals.sagepub.com/home/jcbfm
SAGE

Up-regulation of Wnt/β-catenin expression is accompanied with vascular repair after traumatic brain injury

Arjang Salehi[1,2], Amandine Jullienne[2], Mohsen Baghchechi[2], Mary Hamer[2], Mark Walsworth[2], Virginia Donovan[2], Jiping Tang[4], John H Zhang[4,5,6], William J Pearce[4,7] and Andre Obenaus[1,2,3]

Abstract

Recent data suggest that repairing the cerebral vasculature after traumatic brain injury (TBI) may help to improve functional recovery. The Wnt/β-catenin signaling pathway promotes blood vessel formation during vascular development, but its role in vascular repair after TBI remains elusive. In this study, we examined how the cerebral vasculature responds to TBI and the role of Wnt/β-catenin signaling in vascular repair. We induced a moderate controlled cortical impact in adult mice and performed vessel painting to visualize the vascular alterations in the brain. Brain tissue around the injury site was assessed for β-catenin and vascular markers. A Wnt transgenic mouse line was utilized to evaluate Wnt gene expression. We report that TBI results in vascular loss followed by increases in vascular structure at seven days post injury (dpi). Immature, non-perfusing vessels were evident in the tissue around the injury site. β-catenin protein expression was significantly reduced in the injury site at 7 dpi. However, there was an increase in β-catenin expression in perilesional vessels at 1 and 7 dpi. Similarly, we found increased number of Wnt-GFP-positive vessels after TBI. Our findings suggest that Wnt/β-catenin expression contributes to the vascular repair process after TBI.

Keywords

Angiogenesis, brain recovery, brain trauma, regeneration and recovery, vascular biology

Received 18 April 2017; Revised 18 September 2017; Accepted 23 October 2017

Introduction

Traumatic brain injury (TBI) is a serious clinical problem that is associated with long-term neurological deficits. Emerging research suggests that the cerebral vasculature is one of the major contributors to TBI-related disabilities.[1,2] An insult to the brain damages cerebral vessels and often leads to secondary injury. For example, patients with severe TBI experience acute reductions in cerebral blood flow that gradually resolves over the course of several days to weeks.[3] Although improved guidelines for the management of TBI patients have been introduced, they have been largely ineffective in reducing the incidence of post-injury ischemic episodes.[4] Thus, a better understanding of how the cerebral vasculature responds following TBI could provide critical insight into secondary effects

[1]Cell, Molecular and Developmental Biology Program, University of California, Riverside, CA, USA
[2]Department of Pediatrics, Loma Linda University, Loma Linda, CA, USA
[3]Department of Pediatrics, University of California, Irvine, CA, USA
[4]Department of Physiology and Pharmacology, School of Medicine, Loma Linda University, Loma Linda, CA, USA
[5]Department of Anesthesiology, School of Medicine, Loma Linda University, Loma Linda, CA, USA
[6]Department of Neurosurgery, School of Medicine, Loma Linda University, Loma Linda, CA, USA
[7]Center for Perinatal Biology, Loma Linda University, Loma Linda, CA, USA

Corresponding author:
Andre Obenaus, Department of Pediatrics, Loma Linda University, Coleman Pavilion, Room A-1120, 11175 Campus Street, Loma Linda, CA 92354, USA.
Email: aobenaus@llu.edu

and lead to development of new therapies designed to enhance vascular repair.

The time course of vascular repair after TBI has been ill-defined. Injured vessels undergo repair through sprouting angiogenesis (formation of new capillaries from existing vessels). Several studies have suggested that TBI elicits gross vascular injury that is subsequently followed by slow repair over the course of several weeks.[5,6] The degree of vascular repair is dependent on the severity of the TBI.[5] Interestingly, secondary complications (i.e. hypoperfusion) are observed once the vascular network has repaired, which may suggest deficits in the repaired vessels.[7] At present, there are no studies that have comprehensively investigated the spatial and morphological changes of the brain vasculature after TBI.

Several putative mechanisms may be responsible for vascular repair after TBI. Vascular endothelial growth factor (VEGF) has been evaluated in several studies.[8,9] However, VEGF treatment appears to exhibit adverse side effects making it a poor candidate for future therapeutics.[10] One alternative and unexplored mechanism is the Wnt/β-catenin cascade, which plays a major role in embryonic vascular development. This pathway regulates many aspects of the vascular repair processes, including angiogenesis, vascular sprouting, blood–brain barrier formation, and arterial-venous specification.[11–15] Additionally, studies in other vascular-related injuries (stroke, hindlimb ischemia and neointimal hyperplasia) demonstrated that the components of Wnt/β-catenin pathway have angiogenic functions.[16–18]

The Wnt/β-catenin pathway has recently been explored in TBI unrelated to the cerebral vasculature. Studies have shown contrasting results, with several reporting up-regulation of β-catenin after TBI,[19,20] while others showing a dramatic reduction.[21] In damaged tissue, Wnt factors are thought to promote proliferation and differentiation of stem and progenitor cells. After TBI, the Wnt/β-catenin pathway has been linked to important repair processes, most notably astrogliosis and neurogenesis.[19,22,23] It is unclear what role the Wnt/β-catenin signaling plays in vascular repair after TBI.

The objective of our study was to evaluate how the cerebral vessels respond in the course of seven days following a moderate TBI. The second objective was to assess what role the Wnt/β-catenin signaling plays in the vascular repair process. We hypothesized that Wnt/β-catenin signaling is associated with repair of the injured vasculature after TBI. We utilized a controlled cortical impact (CCI) mouse model to induce a moderate TBI which lead to gross injury to the cortical vessels. We utilized a novel vessel painting technique to label the cerebral vessels in the whole brain and assessed vascular alterations at specific time points after TBI. We assessed β-catenin inside blood vessels around the lesion and utilized a Wnt transgenic mouse line to monitor Wnt gene expression. In our study, we found that TBI led to a rapid up-regulation of β-catenin expression and activation of Wnt genes in blood vessels that coincided with vascular repair. These results suggest that Wnt/β-catenin expression contributes to vascular repair following TBI and represents a potential target for future therapeutics.

Material and methods

All animal experiments and care complied with federal regulations and were approved by the Institutional Animal Care and Use Committee of Loma Linda University according to Guide For the Care and Use of Laboratory Animals (Eighth edition). Experiments received ethical approval from the LLU IACUC under the protocol numbers 8130051 and 8150023. Animal reporting is according to ARRIVE guidelines.

Animals

Male C57BL/6 mice (6–8 weeks, 25–30 g) were purchased from Jackson Laboratory. Male transgenic TCF/Lef:H2B-GFP mice (6–8 weeks, 25–30 g) were on a C57BL/6 background and were purchased from Jackson Laboratory. Animals were group housed and kept in a temperature-controlled animal facility on a 12-hour (h) light/dark cycle with free access to food and water. Home cages contained standard cob bedding. Animals were randomly assigned to three groups: control, sham, or TBI. Following brain injury, animals underwent vessel painting, Western blot, or immunohistochemistry. All animals were sacrificed at 0.5, 1, 3, or 7 days post injury (dpi). Each experiment was performed by investigators blinded to the treatment/subject.

TBI

A CCI model of moderate brain injury was utilized as described previously.[24] Briefly, mice were anesthetized with isoflurane (3% induction, 1–2% maintenance) using isoflurane vaporizer (VetEquip Inc., Pleasanton, CA, USA). Anesthetized mice were placed in a stereotaxic frame and body temperature was maintained at $37 \pm 1^{\circ}C$ with a heating pad during the surgery. A midline incision of the skin was made to expose the skull and a 5 mm craniotomy was carefully performed on the right hemisphere to expose the cortex (between Lambda and Bregma). A moderate CCI (1.5 mm depth, 3 mm diameter, 2.0 m/s speed, 200 ms dwell time) was delivered using an electromagnetically driven piston (Leica Microsystems Company,

Richmond, IL). CCI procedure resulted in visible hemorrhage that gradually resolved in a few minutes. The craniotomy site was not sealed and skin was sutured. After surgery, buprenorphine (0.01 mg/kg, intramuscular) was administered to minimize pain. Animals were monitored daily following the procedure. Sham animals underwent the exact procedure without cortical impact. In a small cohort of sham animals, we noted small degree of hemorrhage which was due to the craniotomy procedure. Control animals underwent anesthesia for the identical period of time (30 min) as well as the buprenorphine injection. Control and sham animals were euthanized after three days.

Vessel painting procedure

This technique uses a carbocyanine dye (1,1′-dioctadecyl-3,3,3′,3′-tetramethylindocarbocyanine perchlorate, DiI, Life Technologies, Carlsbad, CA) that binds to the lipid membranes, thereby labeling the vasculature of the entire brain.[25] Mice were assigned into three groups: Sham, TBI 1 dpi, and TBI 7 dpi (19 total, n = 6–7/group). Mice were anesthetized with ketamine (90 mg/kg) and xylazine (10 mg/kg). Vessel painting was performed by cardiac injection of DiI (0.3 mg/mL in PBS containing 4% dextrose, total volume 500 μL) into the left ventricle followed by perfusion with 10 mL of phosphate buffer saline (PBS) and then 20 mL of 4% paraformaldehyde (PFA). Extracted brains were then post-fixed in 4% PFA for 24 h and stored in PBS until imaging. Success of vessel painting was confirmed based on visualized inspection of the brain parenchyma where a uniform pink stain demonstrated vascular labeling providing excellent definition of large and small cortical and subcortical vessels. Animals with uneven staining of the vessels were excluded. Axial and coronal brain images were then obtained using a BZ-X700 Keyence microscope (Keyence Corp, Osaka, Japan). Axial views of the brain were obtained using 2× magnification and 1 mm depth of field (25.2 μm pitch, 40 slices). For coronal images, brains were sliced at the lesion site, 5 mm away from the olfactory bulbs and imaged using 2× magnification and 0.75 mm depth of field (25.2 μm pitch, 30 slices).

Vessel painting analysis

Quantitative analysis of the labeled vessels was performed as described previously on whole brain axial and coronal views.[25] Regions of interest (ROIs) were drawn around the ipsilateral and contralateral hemisphere on 2× axial and coronal images. Perilesional area analysis was performed using a 1.5 mm diameter ROI encompassing the lesion. ROIs were drawn around each lesion and then were expanded by 1.5 mm to encompass the perilesional area. Angiotool analysis was performed on each ROI to assess vessel characteristics, including vessel density, junction number, and average vessel length.[26]

Western blotting

Western blot assays were performed using controls in lieu of sham animals as the craniotomy results in small alterations to the cortical surface[27] and affects expression of β-catenin in the brain (data not shown). Mice were assigned into five groups: Controls (n = 13), TBI 0.5 (n = 6), 1 (n = 7), 3 (n = 6), and 7 dpi (n = 6) (38 total). The animals were sacrificed by transcardial perfusion with PBS. Extracted brains were cut into four quadrants (between the midline and Bregma) and the quadrants containing the injury site were processed to extract cytoplasmic and nuclear proteins (Nuclear extraction kit, EMD Millipore, Temecula, CA). Protein concentration was determined using a Bradford assay (Thermo Scientific, Rockford, IL). Protein (8 or 10 μg) was subjected to electrophoresis on 4–12% Sodium Dodecyl Sulfate PolyAcrylamide Gel Electrophoresis gels and transferred onto polyvinylidene difluoride membranes. Immunoblots were probed with the following antibodies: rabbit anti-β-catenin, rabbit anti-GAPDH, rabbit anti-Lamin B1 (1:2000), rabbit anti-Cyclin D1 (1:10,000), or anti-Wnt5a (1:200) (all antibodies from Abcam, Cambridge, MA). Secondary incubations were performed with anti-rabbit DyLight 800 (1:2500, Thermo Fisher, Rockford, IL, USA) and anti-mouse IRDye 680 (1:2500, LI-COR, Lincoln, NE, USA) antibodies and incubated for 2 h. Bands were visualized using an infrared scanner (Odyssey, LI-COR). Image Studio Lite (LI-COR) was used for densitometry analysis, and band intensities were normalized to their respective loading controls.

Immunohistochemistry

Mice were assigned into three groups: Controls, TBI 1 dpi, and TBI 7 dpi (n = 3–4/group). All animals appeared healthy before sacrificing. C57BL/6 (12 total) and transgenic TCF/Lef:H2B-GFP (12 total) mice used for immunohistochemistry were sacrificed by transcardial perfusion with PBS and 4% PFA. Following post-fixation, brains were cryoprotected in 30% sucrose solution for 24 h. Brains were embedded in Tissue-Tek OCT compound (Sakura Finetek, Torrance, CA, USA) and frozen on dry ice. Coronal sections were obtained using a cryostat (Leica Biosystems, Nussloch, Germany) at a 20 μm thickness and collected on Superfrost Plus® (Fisher Scientific,

Pittsburg, PA) microscope slides. Tissue sections were blocked with 2% bovine serum albumin (BSA, Sigma Aldrich, St Louis, MO, USA) solution for 1.5 h. Primary antibodies used were: anti-β-catenin (1:100, Abcam, Cambridge, MA), anti-Sox17 (1:100, Abcam), anti-Von Willebrand Factor (vWF, 1:200, Abcam), anti-GFAP (1:500, Millipore, Billerica, MA), anti-NeuN (1:400, Millipore), and anti-Iba1 (1:400, Wako, Richmond, VA). DyLight 594-labeled tomato-lectin (T-lectin, 1:200, Vector Laboratories, Burlingame, CA) and Isolectin B4 (IB4, 1:50, Sigma Aldrich) were used to label the blood vessels. Primary antibodies or markers were incubated in antibody solution (0.5% BSA + 0.5% Triton X) overnight or for 72 h for IB4. Appropriate secondary antibodies (all from Invitrogen, Eugene, OR, USA) were incubated in antibody solution for 1.5 h. Slides were coverslipped with Vectashield mounting medium (Vector Laboratories, Burlingame, CA, USA) containing DAPI as a nuclear counterstain.

β-catenin and IB4 expression analysis

Mouse brain sections from control and TBI animals were labeled with β-catenin antibody and T-lectin. Vessel-painted brain sections DiI from sham and TBI 7 dpi animals were labeled with IB4 antibody. Images were blinded before analysis. For each animal, two images were randomly captured with a fluorescence microscope (Keyence BZ-X700) in the cortical tissue surrounding the injury site at 20× magnification. Images were converted to grayscale and background was reduced by adjusting threshold values using ImageJ software. Images were overlaid (Image calculator, multiply) or subtracted (Image calculator, subtract) in order to measure the amount of co-localized and non-co-localized signal of the β-catenin and T-lectin channels, respectively. Total β-catenin, co-localized intensity, and non-co-localized intensity were calculated, and integrated density values were used for analysis. Total IB4 and IB4-DiI colocalized integrated density were also calculated.

Quantification of Wnt-GFP expressing cells and vessels

TCF/Lef:H2B-GFP mouse brain sections at the level of the injury were stained with T-lectin. Two images were randomly captured from the cortical tissue surrounding the injury site at 20× magnification. GFP-positive nuclei and vessel segments were counted using the cell counting plugin in ImageJ. GFP-positive vascular cells were selected according to their endothelial cell-like morphology (oval nuclei, scant cytoplasm, and elongated cell outline) and location in the vessel. A single vessel segment was selected if it was present between two vessel junction points, two open endpoints, or a junction and open endpoint. GFP-positive vascular cells, positive vessel segments, and total vessel segments were calculated as a total of the two images. Immunohistochemical analyses were performed blindly and interpreted independently by two experimenters.

Statistics

Investigators were blinded to experimental conditions for all analyses. All measurements and analysis were performed without knowledge of the groups. One-way analysis of variance (ANOVA), with a post-hoc Tukey test, was used for comparison of vessel characteristics between hemispheres and perilesional tissue. One-way ANOVA, with a post-hoc Tukey test, was used for comparison of β-catenin and Cyclin D1 protein levels at multiple time points. Student t-test was used for comparison of Wnt5a protein levels. The data for the parametric tests showed a normal distribution and passed the Shapiro-Wilk normality tests. Student t-test, with Mann-Whitney test, was used for comparison of IB4 and DiI expression, and one way ANOVA, with Kruskal-Wallis test, was used for comparison of Wnt-GFP cells and positive vessel segments at multiple time points. All analyses was performed using GraphPad Prism 5.0 (GraphPad, San Diego, CA). Outliers were identified if they were below or above 1.5 times the interquartile range. All error bars are presented as standard error of mean (SEM). Statistical significance was noted at $*p < 0.05$, $**p < 0.01$, or $***p < 0.001$.

Results

Assessment of the cortical vasculature

We developed a novel vessel painting protocol that labels the whole brain vasculature. Vessel-painted brains revealed excellent staining of the cortical and subcortical vessels (Figures 1(a) and 2(a)). Thus, we utilized this technique to visualize vessel alterations within the brain after a moderate TBI. All animals appeared healthy before the procedure. A craniotomy alone in the sham group showed minimal disruption of the vessels. The 1-day post-injury (dpi) group showed clear vascular loss at the site of the injury which extended to the outer perimeters as previously reported[28] (Figure 1(b)). Conversely, the 7 dpi group revealed revascularization around the injury site (Figure 1(b)). The majority of these new vessels appeared to originate from the perilesional tissue, radiating towards the injury site (Figure S1). Irregular, disorganized, and clearly disrupted vessels were also evident within the base of the injury site.

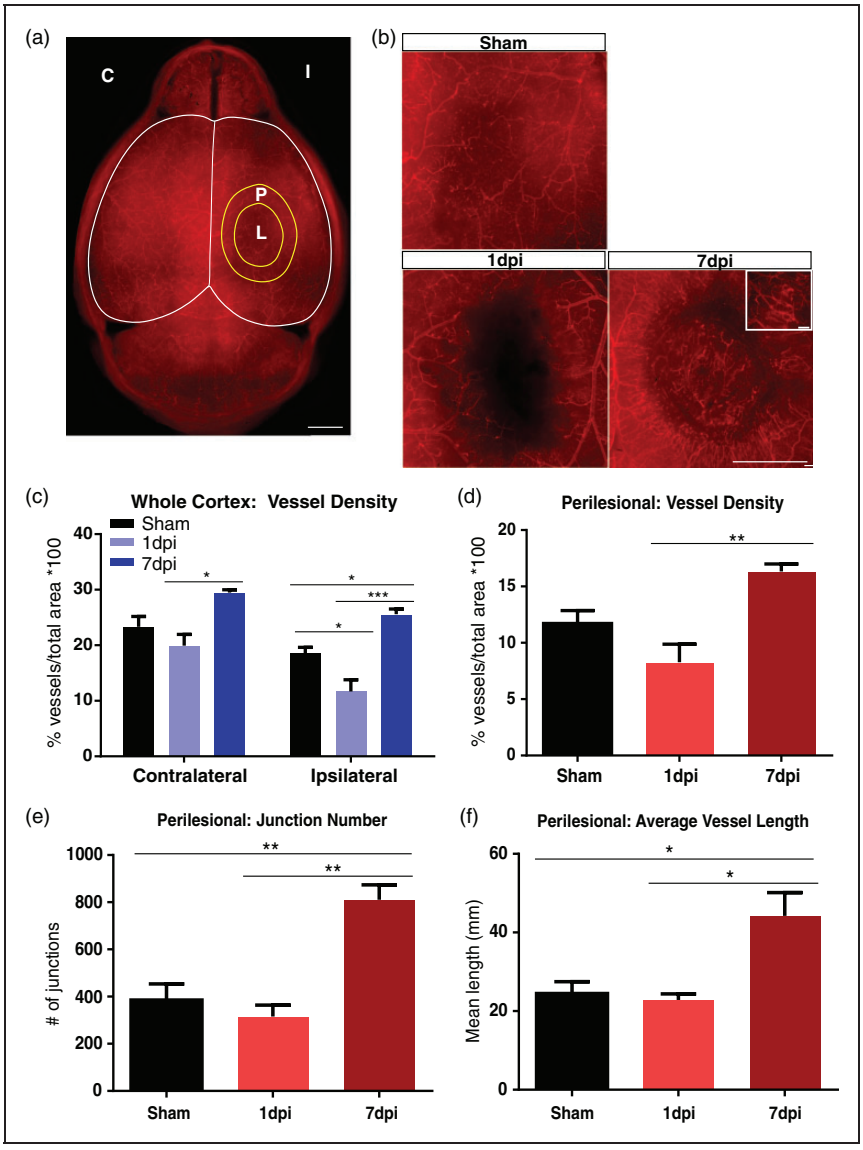

Figure 1. TBI results in vascular injury followed by repair. (a) Axial view of a vessel-painted brain from a Sham animal illustrating the dense vascular plexus. Analysis on the ipsilateral (I), contralateral (C) hemispheres, and perilesional tissue (P) around the lesion (L) was undertaken. Scale bar = 1000 μm. (b) Representative images from Sham, 1 dpi, and 7 dpi groups. Sham animals exhibited minor vascular disruptions due to the craniotomy. In the 1 dpi group, there was a clear disruption of the vessels that extended beyond the impact site. In contrast, the 7 dpi group showed the presence of newly formed vessels around the impact site. The inset illustrates these new vessels at high magnification. Scale bar = 1000 μm, 100 μm (insert). (c) Vascular analysis of the ipsilateral hemisphere demonstrating a reduction in vessel density (one-way ANOVA, $p < 0.05$) in 1 dpi group compared to shams, while the 7 dpi group showed a significant increase in vessel density (one-way ANOVA, $^{***}p < 0.001$, $^{*}p < 0.05$) compared to the 1 dpi and sham groups. The contralateral hemisphere also exhibited a reduction in vessel density (not significant) at 1 dpi compared to the sham group. Interestingly, the 7 dpi group showed a significant increase in vessel density (one-way ANOVA, $^{*}p < 0.05$) compared to the 1 dpi group with no change compared to shams. (d) Vascular analysis of perilesional tissue revealing a significant increase in vessel density (one-way ANOVA, $^{**}p < 0.01$) in the 7 dpi compared to the 1 dpi group. (e) Analysis of the perilesional tissue revealing a significant increase in the number of junctions (one-way ANOVA, $^{**}p < 0.01$) in the 7 dpi compared to 1 dpi and sham groups. (f) Similarly, we observed a significant increase in average vessel length (one-way ANOVA, $^{*}p < 0.05$) in the 7 dpi compared to 1 dpi and sham groups.

In order to determine the degree of vessel alterations after TBI, we undertook vascular analysis to evaluate vessel density, number of junctions, and average vessel length (Figure 1(c) to (f)). The sham group (n = 6/6) showed a reduction in vessel density in the ipsilateral hemisphere compared to the contralateral hemisphere (not significant), which was the result of the craniotomy. Vessel density in the ipsilateral hemisphere was

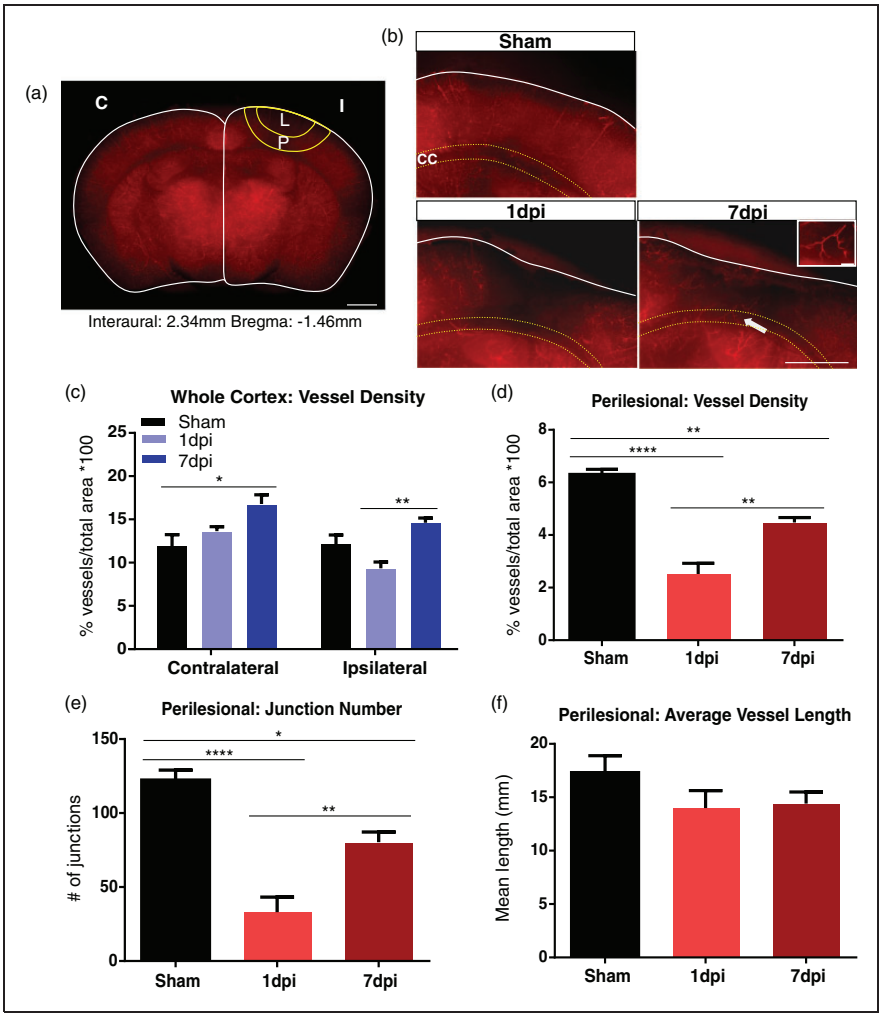

Figure 2. Coronal assessment of vessel-painted vasculature. (a) Coronal view of a vessel-painted sham animal illustrating staining of the cortical and subcortical vasculature. ROIs in the ipsilateral (I), contralateral (C) hemispheres, and perilesional tissue (P) encompassing the lesion (L) were undertaken. Scale bar = 1000 μm. (b) Representative images of sham, 1 dpi, and 7 dpi animals. The sham group exhibited minor loss of vessel density, whereas the 1 dpi group had extensive vascular loss of the cortical vessels that extended to the corpus callosum (CC, yellow dotted line). The 7 dpi group revealed newly formed vessels radiating toward the impact site (arrow). High magnification image of designated vessel is present in the insert. Scale bar = 200 μm, 100 μm (insert). (c) Vascular analysis of the ipsilateral hemisphere demonstrating a reduction in vessel density (not significant) at 1 dpi, while the 7 dpi group showed a significant increase in vessel density (one-way ANOVA, ** $p < 0.01$) compared to the 1 dpi group. Analysis of the contralateral hemisphere demonstrated an increase in vessel density (one-way ANOVA, *$p < 0.05$) in 7 dpi group compared to shams. (d) Vascular analysis of the perilesional tissue revealing a significant increase in vessel density (one-way ANOVA, **$p < 0.01$) in the 7 dpi compared to the 1 dpi group. Vessel density in the 7 dpi group (one-way ANOVA, **$p < 0.01$) was significantly reduced compared to the sham group. (e) Similarly, we observed a significant increase in the number of junctions (one-way ANOVA, **$p < 0.01$) in the 7 dpi compared to the 1 dpi group. Number of junctions in the 7 dpi group (one-way ANOVA, *$p < 0.05$) was significantly reduced compared to the Sham group. (f) Vessel length at 1 and 7 dpi showing a reduction compared to the shams, but it did not reach significance.

decreased at 1 dpi by 36.7% compared to shams ($p < 0.05$), which was followed by a 118.9% increase at 7 dpi ($p < 0.001$) (Figure 1(c)). The 1 dpi group ($n = 5/6$, 1 outlier) exhibited decreased total vessel density of 11.69 ± 2.08 (mean ± SEM) compared to 25.59 ± 0.93 in the 7 dpi group ($n = 4/5$, 1 outlier). Interestingly, the contralateral hemisphere showed a similar 48% increase in vessel density at 7 dpi ($p < 0.05$) compared to 1 dpi (Figure 1(c)). The 1 dpi group had a total vessel density of 19.93 ± 2.01 compared to 29.49 ± 0.51 in the 7 dpi group.

We next examined the vessel differences in the perilesional tissue (Figure 1(a)). The sham group ($n = 6/6$) showed no significant difference in any vessel parameters when comparing both hemispheres. The 1 dpi group ($n = 5/6$) showed a reduction in vessel density

compared to the sham group, but this did not reach significance (no statistical differences appeared in any of the other parameters). We observed a 97.1% increase in vessel density ($p < 0.01$), 157.0% increase in number of junctions ($p < 0.01$), and 93.7% increase in average vessel length ($p < 0.05$) at 7 dpi ($n = 4/5$, 1 outlier) compared to 1 dpi (Figure 1(d) to (f)). Thus, these results suggest that there is a global increase in the vasculature following TBI across both hemispheres by 7 dpi.

Assessment of the subcortical vasculature

To further assess the effects of cortical injury to the vasculature, we analyzed coronal sections of vessel-painted brains (Figure 2(a)). The 1 dpi group revealed loss of the cortical vessels that extended to the corpus callosum (Figure 2(b)), and similar to the whole brain axial data (see above), the 7 dpi group exhibited increased vascularization around the injury site (Figure 2(b)). Newly formed vessels appeared to extend from the surrounding tissues radiating toward the injury site. Similar to the axial cortical findings, sham mice showed minor injury to the cortical vessels.

Vascular analysis was performed on the coronal sections to quantify vessel characteristics. There was no significant difference in vessel density between the hemispheres. Vessel density in the ipsilateral hemisphere exhibited a non-significant decrease at 1 dpi ($p = 0.12$), followed by a significant 56.5% increase at 7 dpi ($p < 0.01$) (Figure 2(c)). The 1 dpi group ($n = 5/6$, 1 outlier) exhibited a total cortical vessel density of 9.33 ± 0.74 compared to 14.61 ± 0.56 in the 7 dpi group ($n = 5/5$). Vessel density in the contralateral tissue was increased by 41.6% at 7 dpi ($p < 0.05$) compared to the shams (Figure 2(c)). The sham group ($n = 6/6$) had a total vessel density of 11.86 ± 1.38 compared to 16.79 ± 1.06 in the 7 dpi group.

Analysis of vascular features in the perilesional tissue (Figure 2(a)) found that TBI caused a significant decrease in vessel density and number of junctions at 1 dpi ($p < 0.001$, $n = 5/6$, 1 outlier), followed by 77.9% and 143% increase at 7 dpi ($n = 5/5$) (Figure 2(d) to (f)). Interestingly, both parameters at 7 dpi were still significantly reduced compared to shams ($p < 0.05$, $p < 0.01$, $n = 6/6$). There was no significant difference in average vessel length. Thus, these results suggest that despite robust repair of the cortical vessels, there is a slower temporal repair of vessels within the deeper layers of the cortex.

Newly formed, non-perfusing vessels

While our vessel painting technique labels perfused vessels in the brain, this method does not directly identify new or immature vessels after injury that are non-perfusing. Undamaged and newly formed vessels can be distinguished according to endothelial tip cell morphology and their perfusion status.[29] To investigate this, we further examined our vessel-painted brains and stained with IB4 to label all the blood vessels, including endothelial tip and stalk cells. The 7 dpi group exhibited an increased number of IB4+/DiI− vessels in comparison to the sham group (Figure 3(a)). Along with having reduced or lack of DiI staining, these vessels appeared thinner and more elongated than normal sham vessels, suggesting that they are likely immature (Figure 3(b)). Furthermore, we observed IB4+ endothelial tip cells extending their filopodia into the extracellular environment that often were not associated with DiI+ vascular components consistent with vascular sprout formation (Figure 3(c)). Quantitative analysis of the perilesional tissue revealed an increase in IB4 expression in the 7 dpi ($p = 0.09$) compared to the sham group, but this did not reach significance. However, we observed a 31.0% reduction in DiI-expressing IB4+ vessels by 7 dpi ($p < 0.05$) when compared to the shams, indicating that the new vessels are non-perfusing. The sham group ($n = 3/4$, 1 outlier) had a DiI/IB4 colocalized integrated density of 2463 ± 63.69, while the 7 dpi group ($n = 4/4$) had 1700 ± 202.40. Thus, these data provide further evidence for vascular regrowth after TBI.

Changes in β-catenin expression profile

The Wnt/β-catenin signaling pathway is tightly regulated by the protein β-catenin. Upon activation, β-catenin escapes degradation where it accumulates in the cytoplasm and translocates into the nucleus where it complexes with T-cell-specific transcription factor/lymphoid enhancer-binding factor (TCF/LEF) to promote transcription of Wnt target genes. We hypothesized that TBI activates the Wnt/β-catenin signaling pathway to initiate vascular repair. To test this hypothesis, we measured cytoplasmic and nuclear β-catenin protein levels in the injury site over the course of seven days after injury. The animals in the control group showed no change in cytoplasmic and nuclear β-catenin levels over seven days following anesthesia treatment. We found that cytoplasmic β-catenin protein levels were reduced to 93.9% by 7 dpi ($p < 0.05$) when compared to 1 dpi (Figure 4(a) and (b)). The 1 dpi group ($n = 5/7$, 2 outliers) had a normalized cytoplasmic β-catenin level of 92.15 ± 20.55 compared to 5.59 ± 3.52 for the 7 dpi group ($n = 5/6$, 1 outlier). Similarly, there was a 35.7% reduction in nuclear β-catenin protein levels by 7 dpi ($p < 0.05$) (Figure 4(a) and (c)). The 1 dpi group had normalized nuclear β-catenin levels of 84.01 ± 5.17 compared to 54.03 ± 8.30 for the 7 dpi group.

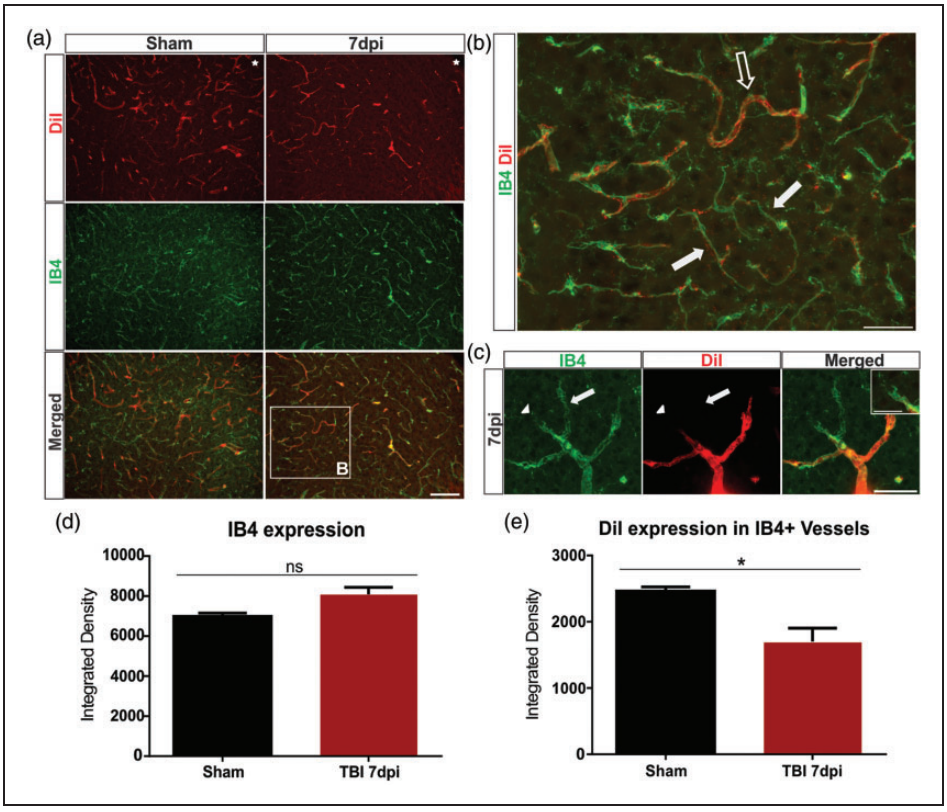

Figure 3. Identification of perfused and newly formed blood vessels in the cortex. (a) Sham animals showed uniform vessel staining with DiI in coronal sections (see Figure 2), whereas the 7 dpi group exhibited a reduction in labeled vessels adjacent to the injury site (top panel). Similarly, in shams, there was a uniform staining of IB4+ vessels with an apparent reduction in the 7 dpi group. Interestingly, there appeared to be an increase in co-localized DiI and IB4+ vessels in the sham group, with little co-localization in the 7 dpi group. The boxed area is enlarged in (b). Star indicates region of impact. Scale bar = 100 μm. (b) A IB4+/DiI+ vessel from a 7 dpi mouse (open arrow) that is perfused (DiI+). Immature vessels, IB4+/DiI−, appear narrower and elongated in shape and are likely not fully formed nor perfused (solid arrow). Scale bar = 50 μm. (c) High magnification image of a newly forming vessel branching from an existing vessel. A new vessel is seen sprouting from a pre-existing vessel (arrow). IB4+ endothelial tip cells extend their filopodia into the cortex (arrowhead). Insert illustrates the filopodia of an endothelial tip cell. Scale bar = 25 μm, 15 μm (insert). (d) Analysis of the perilesional tissue revealing an increase in IB4 expression in the 7 dpi (Student t-test, $p = 0.09$) compared to the sham group. (e) Analysis revealing a significant decrease in DiI-expressing IB4 + vessels in the 7 dpi (Student t-test, $^*p < 0.05$) when compared to the sham group.

To assess activation of Wnt genes, we measured the expression of the downstream Wnt target gene Cyclin D1. We found that cytoplasmic Cyclin D1 protein levels were increased at 1 dpi ($p < 0.01$) and peaked at 3 dpi ($p < 0.001$) when compared to 12-h group (Figure 4(d) and (e)). The 3 dpi group ($n = 5/5$) had a normalized Cyclin D1 levels of 203.20 ± 17.2 compared to 80.67 ± 9.37 for the 12-h group ($n = 5/5$) with an increase of 151.9%. Interestingly, Cyclin D1 protein levels were reduced at 7 dpi ($p < 0.05$) when compared to the 3 dpi group. We next tested the expression of non-canonical Wnt5a, which downregulates β-catenin-induced gene expression.[30] Wnt5a protein levels increased 141.9% at 7 dpi ($p < 0.05$) when compared to 1 dpi group (Figure 4(f) to (g)). The 7 dpi group ($n = 5/5$) had a normalized Wnt5a levels of 150.90 ± 26.78 compared to 62.06 ± 20.24 for the 1 dpi group ($n = 4/5$, 1 outlier). Thus, these data suggest that β-catenin levels are reduced at the injury site at 7 dpi and are likely inhibited by the non-canonical Wnt pathway.

We investigated β-catenin expression in blood vessels in the injured cortical tissue by staining for β-catenin and the vascular marker T-lectin. The control group exhibited uniform β-catenin expression throughout the cortex, where β-catenin-expressing cells were primarily non-vascular and seen adjacent to the vessels (Figure 5(a)). After TBI at 1 dpi and 7 dpi, we observed a dramatic reduction in β-catenin expression around the injured cortex. Interestingly, β-catenin expression was specifically up-regulated in cortical vessels (Figure 5(a)). Quantitative analysis revealed a gradual

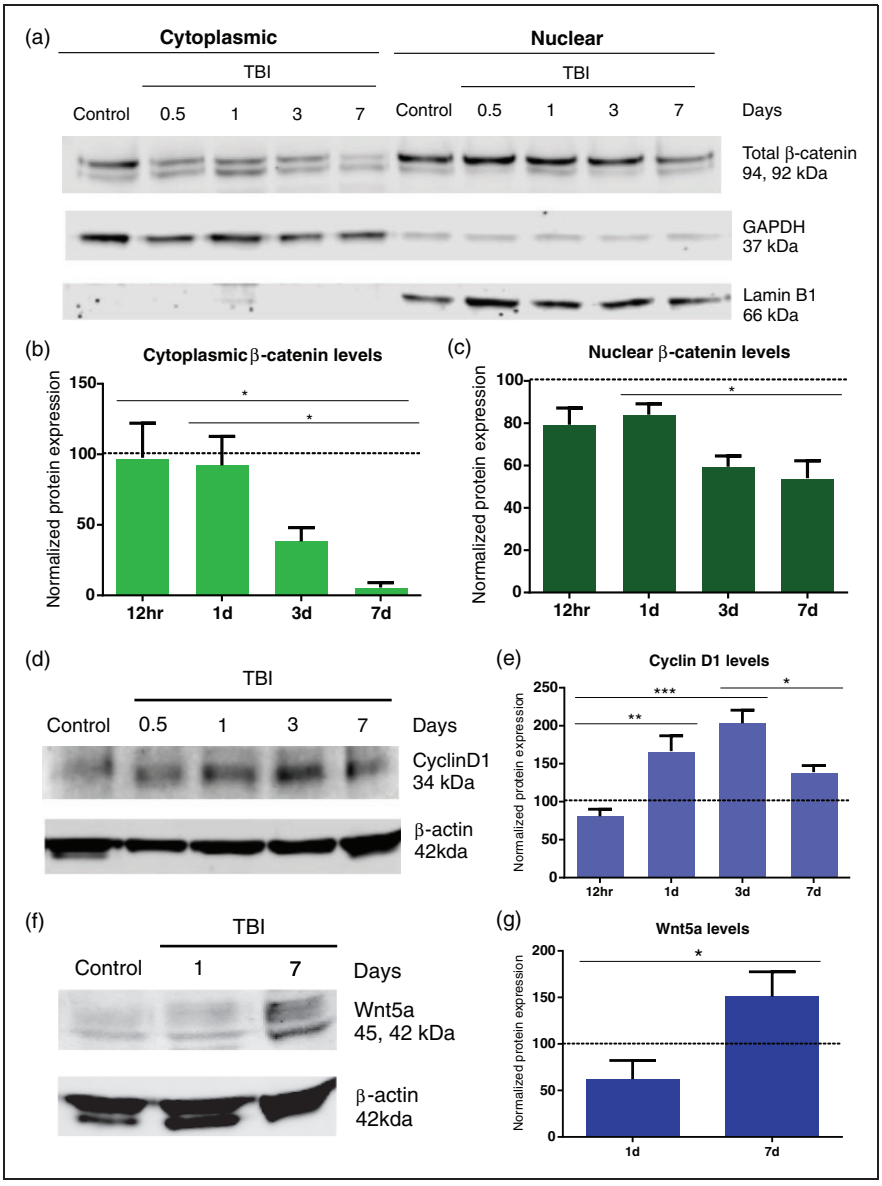

Figure 4. Temporal decrease in β-catenin levels after TBI. (a) Western blots revealing a gradual decrease in cytoplasmic and nuclear β-catenin protein levels over a time course of 7 d after injury. Control animals showed no changes in β-catenin expression during the 7 d time frame. GAPDH was used as cytoplasmic loading control. Lamin B1 was used as a nuclear loading control; 8 μg loaded per well. (b) Densitometric analysis showing a significant decrease in cytoplasmic β-catenin levels (one-way ANOVA, *$p < 0.05$) at 7 dpi compared to the 12 h and 1 dpi groups. (c) Similarly, there was a significant decline in nuclear β-catenin levels (one-way ANOVA. *$p < 0.05$) in the 7 dpi compared to 1 dpi group. Control ($n = 13$), TBI 12 h ($n = 6$), 1 dpi ($n = 7$), 3 dpi ($n = 6$), and 7 dpi ($n = 6$) group. (d) Western blot revealed that Cyclin D1 protein levels peak by 3 dpi followed by reduction at 7 dpi. β-actin was used as cytoplasmic loading control; 10 μg loaded per well. (e) Densitometric analysis demonstrating a significant increase in Cyclin D1 levels at 1 and 3 dpi (one-way ANOVA, **$p < 0.01$, ***$p < 0.001$) when compared to the 12-h group. Expression peaked at 3 dpi. There was a significant decline in Cyclin D1 levels at 7 dpi (one-way ANOVA, * $p < 0.05$) compared to the 3 dpi. (f) Western blot revealing an increase in Wnt5a protein levels at 7 dpi compared to 1 dpi. β-actin was used as cytoplasmic loading control. 10 μg loaded per well. (g) Densitometry analysis showing a significant increase in Wnt5a levels at 7 dpi (Student t-test, *$p < 0.05$) when compared to 1 dpi group.

reduction in β-catenin expression over the course of seven days after injury ($p < 0.001$, control $n = 4/4$. TBI 7 dpi $n = 4/5$, 1 outlier) (Figure 5(b)), consistent with our earlier findings (Figure 4(a) to (c)). Despite the local decrease, β-catenin expression in T-lectin+ vessels was significantly increased by 1 and 7 dpi ($p < 0.05$, TBI 1 dpi $n = 4/4$, $p < 0.001$) in comparison to controls (Figure 5(c)). Furthermore, TBI groups showed a reduction in T-lectin density compared to control groups. Together, these data indicate that

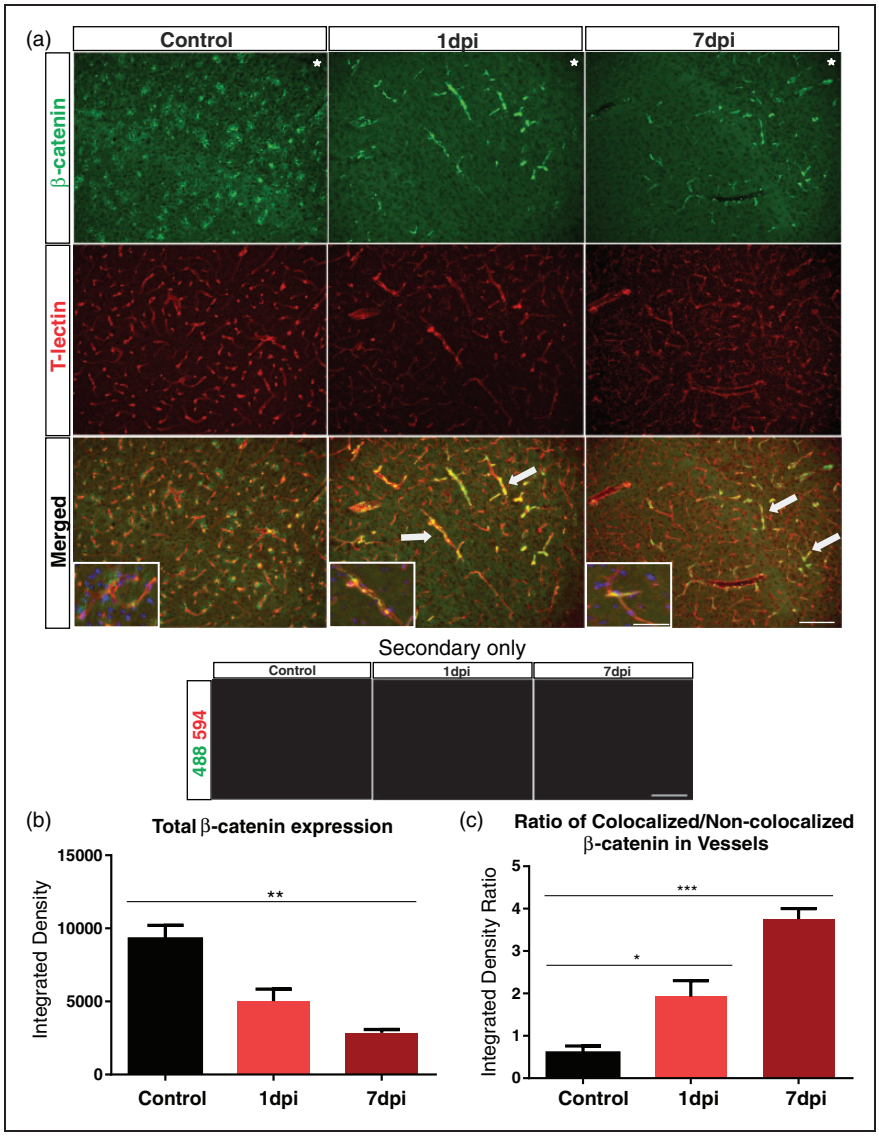

Figure 5. β-catenin is up-regulated in cortical vessels after TBI. (a) Immunohistochemical images from control, 1 and 7 dpi groups. The controls exhibited β-catenin uniform expression in the cortex whereas there was a dramatic loss of expression in the 1 and 7 dpi animals. Vascular loss relative to controls was also observed in the 1 and 7 dpi groups (T-lectin). Interestingly, in the control animals β-catenin expression was observed adjacent to vessels stained with T-lectin, whereas 1 and 7 dpi animals clearly demonstrated β-catenin expression inside vascular structures. Note the increased number of β-catenin+/T-lectin+ vessels in the 1 and 7 dpi groups (arrows). No auto fluorescence was observed in the 594 and 488 channels in any of the tissues. High magnification insert with DAPI illustrates β-catenin-expressing cells adjacent to the vessels in the controls groups and β-catenin+ vessels in the 1 and 7dpi groups. Star indicates region of impact. Scale bar = 100 μm, 50 μm (insert). (b) Densitometric analysis of β-catenin expression in the ipsilateral cortex revealing a significant reduction at 7 dpi compared to controls (one-way ANOVA, $^{**}p < 0.01$). (c) Analysis of β-catenin localization revealing a significant increase in β-catenin expression in T-lectin+ vessels (increased colocalized/non-colocalized ratio) at 1 and 7 dpi compared to the controls (one-way ANOVA, $^{*}p < 0.05$, $^{***}p < 0.001$).

while there is a gradual decrease in β-catenin expression after TBI, there is dramatic shift from non-vascular to expression within vascular elements in the cortical tissue.

Expression of Wnt target genes

To assess Wnt gene expression, we utilized a transgenic reporter mouse line (TCF:LEF1:H2B-GFP) that expresses Histone 2B-GFP fusion protein under the control of TCF/LEF response elements. Similar to wild type, TCF:LEF1:H2B-GFP mice showed an identical reduction in β-catenin expression at 7 dpi ($p < 0.05$, $n = 4/4$) when compared to controls ($n = 3/3$) (Figure S2). Mouse brain sections from control and TBI groups were stained with T-lectin, and the perilesional tissue was assessed. The control group had few

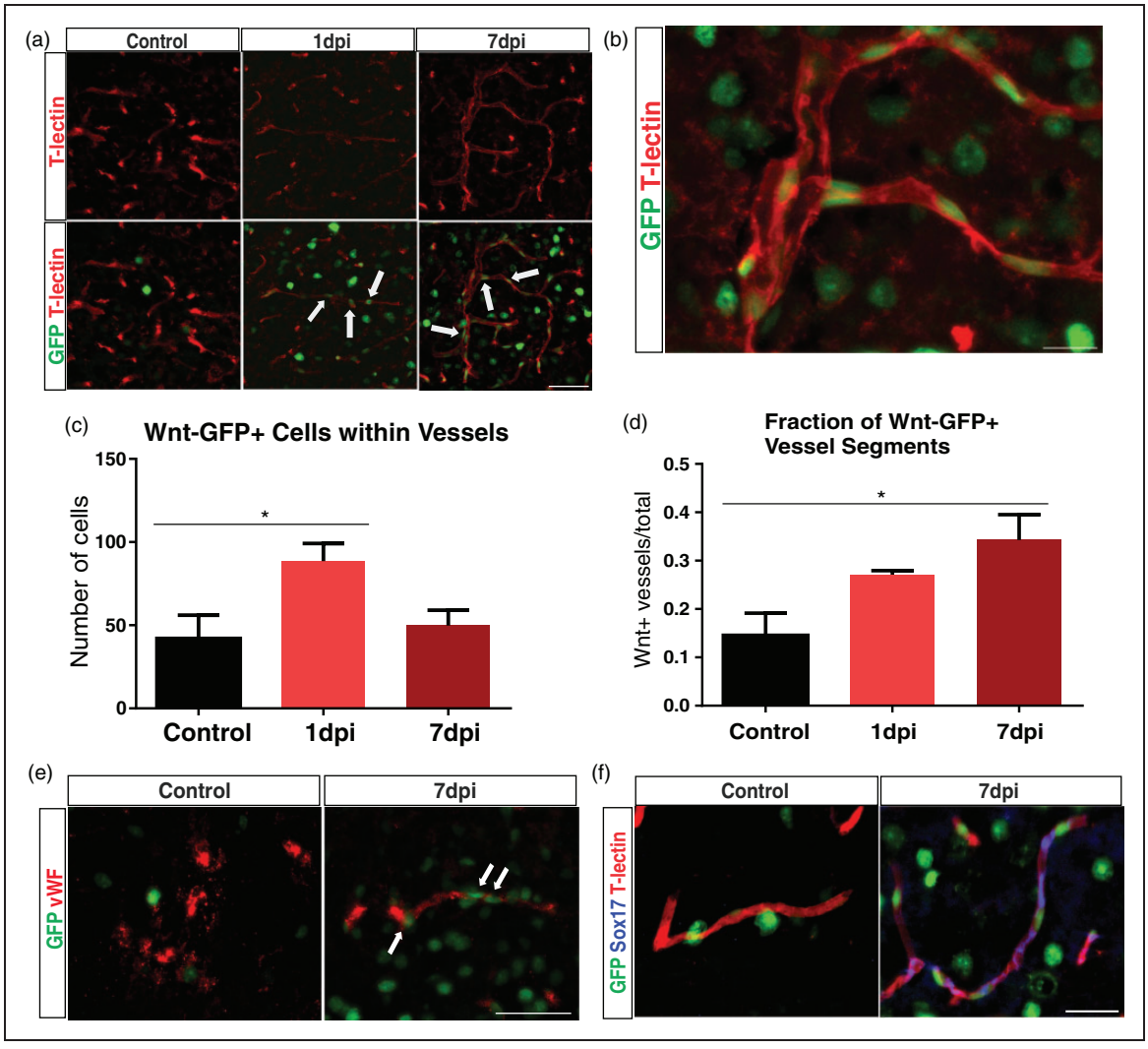

Figure 6. Wnt-GFP-expressing cells are increased inside vascular structures after TBI. (a) We utilized a transgenic mouse line (TCF/LEF:H2B-GFP) to track individual cells with Wnt gene expression. Representative images of control, 1, and 7 dpi groups from the ipsilateral cortex. Few Wnt-GFP vascular cells were seen inside the vessels (T-lectin) in the control group, whereas there was an increase in the 1 and 7 dpi groups (arrows). Scale bar = 50 μm. (b) A vessel from a 7 dpi animal showing Wnt-GFP vascular cells inside blood vessels. Scale bar = 15 μm. (c) Quantitative analysis revealing a significant increase in the number of Wnt-GFP vascular cells at 1 dpi (one-way ANOVA, $*p < 0.05$) which was followed by decrease at 7 dpi (one-way ANOVA, $p = 0.09$). (d) Quantitative analysis revealing a significant increase in Wnt-GFP-positive vessel segments at 7 dpi compared to the controls (one-way ANOVA, $*p < 0.05$). (e) Immunofluorescence of GFP (green) and von Willebrand Factor (vWF; red) in control and 7 dpi group. The control group exhibited heterogeneous vWF expression throughout the brain. In contrast, 7 dpi group showed vWF expression in blood vessels around the impact site. Wnt-GFP vascular cells were found in and around most of these vessels (arrows). Scale bar = 50 μm. (f) Immunofluorescence of Sox17 (blue), GFP (green), and T-lectin (red) in control and 7 dpi group. Sox17 expression is up-regulated in vessels after 7 dpi and colocalizes with GFP+ vessels in Wnt reporter mice. Scale bar = 50 μm.

Wnt-GFP vascular cells inside vessels with most positive cells adjacent to the vessel wall. In contrast, TBI 1 dpi and 7 dpi groups revealed a profound increase in Wnt-GFP vascular cells inside cortical vessels (Figure 6(a) and (b)). Quantitative analysis confirmed a 110.7% increase in Wnt-GFP vascular cells within vessels at 1 dpi ($p < 0.05$, $n = 4/4$) followed by a decline to control levels by 7 dpi ($p = 0.07$, $n = 4/4$) (Figure 6(c)). Control mice ($n = 3/3$) had 42.00 ± 14.01 GFP-positive cells, whereas the 1 dpi group had 88.50 ± 10.65. We also quantified the number of vessel segments that showed Wnt-GFP positivity. Analysis revealed a 126.7% increase in Wnt-GFP-positive vessel segments at 7 dpi ($n = 4/4$) compared to the controls ($n = 3/3$) (Figure 6(d)). Controls had 0.15 ± 0.05 GFP-positive vessels, whereas the 7 dpi group had 0.34 ± 0.05. There was an increase in Wnt-GFP-positive vessel segments at 1 dpi ($n = 3/4$, 1 outlier), but

this did not reach significance. We also observed increased GFP expression in neurons (NeuN+) and astrocytes (GFAP+) in the injured cortex (Figure S3), which confirms findings from previous studies.[22,23]

We stained with the vascular marker von Willebrand factor (vWF), which preferentially labels activated vessels and has previously been shown to identify newly formed vessels in tumors[31] and in transplanted islets.[32] The control and 1 dpi group showed heterogeneous vWF expression throughout the cortex with limited staining in vascular structures (data not shown for 1 dpi group). Conversely, vWF expression was enhanced in perilesional vessels by 7 dpi. Furthermore, we observed Wnt-GFP-vascular cells in and around vWF+ vessels (Figure 6(e)). We next examined the expression of the Wnt target gene, sex-determining region Y-box 17 (Sox17)[33] after TBI. Compared to the controls, Sox17 expression was increased in vascular structures at 7 dpi and co-localized with Wnt-GFP-positive vessels (Figure 6(f)). Together, these results strongly suggest that Wnt gene expression is enhanced in the vasculature after TBI and it may participate in vascular repair.

Discussion

In this study, we sought to understand how the cerebral vasculature responds after TBI and if Wnt/β-catenin signaling could play a role in vascular repair. We report the following novel findings: (1) TBI results in vascular loss at 1 dpi which was followed by a subsequent increase in vascular features at 7 dpi, (2) immature, non-perfusing vessels were evident around the site of injury at 7 dpi, (3) β-catenin protein levels were reduced in the injury site at 7 dpi, (4) β-catenin expression was increased in perilesional vessels at 1 and 7 dpi, and (5) the number of Wnt-GFP+ vessel segments was increased after trauma. Our findings suggest that Wnt/β-catenin expression contributes to the vascular repair process after TBI.

Preclinical studies using a variety of animal models of TBI have reported repair of injured vessels, albeit abnormal. Park et al.[5] demonstrated that injured cortical vessels were repaired by 14 days after fluid percussion injury. Interestingly, the repaired vasculature in moderate and severely injured animals was abnormal compared to sham animals. Mice that received multiple blast exposures had occluded vessels and narrowed lumens at six months after injury.[34] Similarly, Hayward et al.[7] revealed that vessel density in the ipsilateral cortex was restored by 14 days after fluid percussion injury but with altered cerebral blood flow. We found that there was a decrement at 1 dpi followed by an increase in vessel features at 7 dpi. Our data reveal a more gradual repair of the subcortical vessels within the brain when compared to the cortical vessels on the dorsal surface. The repaired vessels around the injury site appeared irregular and were clearly morphologically different from the uninjured vessels in the sham group. These malformed vessels likely affect how the brain tissue undergoes repair, for example they could impede delivery of oxygen and neurovascular substrates that are necessary for neurogenesis.[35] Additionally, these malformed vessels may prevent clearance of fluid and waste products from the injured tissue and be more susceptible for hemorrhagic progression and other secondary complications.[2] Our results and the work from others suggest that the repaired vasculature is abnormal after TBI, but more work is needed to assess the functionality of these abnormal vessels and how they affect functional outcome.

While previous studies have provided some evidence of vascular repair at the TBI lesion site, they have not assessed changes in the whole brain (hemispheric).[5,7,34] We are the first to report an increase in vascular features in both hemispheres by 7 dpi. These findings strongly suggest a diaschisis effect in which blood vessels from undamaged regions of the brain are activated and have the potential to influence vascular repair. One possible explanation for this effect is up-regulation of angiogenic factors within the blood circulation. Patients with severe TBI have been reported to have increased expression of serum VEGF and angiopoietin-1, two key factors involved in sprouting angiogenesis, by 7–14 dpi.[36,37] These circulating factors likely activate blood vessels throughout the brain and lead to increased vascularization. Another explanation could be diffuse hypoxia, which has been reported in clinical TBIs and can last up to one week after injury.[38] Hypoxia is one the many inducers of sprouting angiogenesis after injury. Studies have shown that chronic hypoxia increases vessel growth in both hemispheres of the rodent brain.[39,40] Thus, angiogenic factors may be up-regulated in diffuse regions of the brain after TBI through a hypoxic-mediated response.

Many studies have utilized a variety of protocols to stain the vasculature in rodents, but these techniques have low efficiency rates, do not effectively stain all the vessels in the whole brain, and have minimal fluorescence.[5,41] In our study, we utilized a novel vessel painting technique to visualize the cerebral vasculature after a moderate TBI. While our technique provides excellent staining of all the blood vessels in the mouse brain (including microvessels), it was difficult to acquire consistent staining across animals. We found that 65% (20 of 31) of mice showed excellent vessel staining, using very stringent criteria (uniform pink staining of entire brain parenchyma and staining of large and small vessels in cortical and deep compartments of the brain) that underwent analysis. We previously utilized a

similar staining procedure in the adult rat after a moderate TBI and found that 70% of rat brains showed excellent vessel staining.[25] An issue with labeling of the vessels may be the result of the high alcohol content (10%) in the DiI solution. Another limitation with our technique is the preferential labeling of DiI to arteries. Previous protocols that used DiI reported high staining of arteries with veins only weakly stained.[42]

Sprouting angiogenesis, or the formation of new capillaries from existing vessels, is an important repair response that is activated after injury. This process is driven by endothelial tip and stalk cells where tip cells migrate into the hypoxic tissue and lead to vessel sprouts, whereas stalk cells proliferate to form the vessel lumen and extend the sprout.[43] Together, these cells form an immature non-perfusing vessel which is later remodeled and matured to form a functional, perfusing vessel.[43] The 7 dpi group showed vessels with narrowed lumens, elongated shapes, and sprouting endothelial tip cells. One interesting finding was that 31.0% of the vessels appeared to have reduced DiI staining which may be a reflection of their immaturity. While these findings suggest that sprouting angiogenesis is occurring around the lesion site, the possibility still exists that these vessels are not de novo but existing vessels that were constricted. We believe that this is unlikely since most instances of vasospasms are transient and occur early after injury, i.e. part of hemostasis.[44–46] Severe vasospasms can last for several weeks after severe TBI and blast injuries but are likely not present in our moderate model at this time point.[45] Another possibility is the obstruction of vessels by microthrombi. Schwarzmaier et al.[46] observed the formation of microthrombi in pial vessels early after moderate TBI (<2 h) leading to reductions in blood flow to the perilesional tissue. The incidence of microthrombi is highest in the acute phases of injury and tends to resolve by one to two weeks.[47] While we cannot rule out the possibility of microthrombi occluding vessels early after TBI, it is unlikely that this will occur at our later time points.

Activation of the Wnt/β-catenin pathway has reported after TBI. However, studies have shown contrasting results with regard to β-catenin expression after TBI.[19–21] The expression profile of β-catenin appears to be dependent on the injury model. We found a reduction in global β-catenin protein levels in the injured brain tissue at 7 dpi. Our results are consistent with Zhang et al.,[21] which found a downregulation of β-catenin protein levels between 3 and 14 days after weight drop injury. Interestingly, despite a reduction in nuclear β-catenin, we noticed increased expression of Cyclin D1 at 1 and 3 dpi, indicating that even low levels of nuclear β-catenin can induce gene activation. It has been suggested that β-catenin fold changes, as opposed to absolute levels, controls Wnt/β-catenin pathway activation.[48] Moreover, when β-catenin is present in the nucleus, it can interact with TCF/LEF family of transcription factors along with a multitude of other transcription factors to enhance or inhibit Wnt/β-catenin signaling.[49] One key inhibitor is the non-canonical Wnt pathway, which can inhibit β-catenin/TCF activity.[30] Others have reported that non-canonical Wnts directly modulate β-catenin by inducing its degradation[50] or redirecting it to the cell membrane.[51] In support of this, we observed increased Wnt5a expression at 7 dpi, indicating that non-canonical Wnt pathway may be involved in suppressing Wnt/β-catenin pathway.

The Wnt/β-catenin signaling pathway is critical in the formation of blood vessels in the central nervous system (CNS).[13,15] The Wnt/β-catenin pathway is robustly activated in CNS vessels during development, but its activity declines in the adult.[52,53] Emerging research suggests that the Wnt/β-catenin pathway is reactivated in blood vessels following CNS injuries and diseases. Lengfeld et al.[54] demonstrated that Wnt/β-catenin pathway partially repairs the blood–brain barrier following multiple sclerosis. Dysfunctional Wnt/β-catenin signaling has also been implicated in aberrant angiogenesis in Huntington's disease.[55] Additionally, this pathway possesses many angiogenic functions in non-CNS injuries. In a vascular balloon injury, β-catenin induces vascular remodeling after injury,[16] and Kim et al.[17] showed that β-catenin modulates angiogenesis and improves vascular function in a mouse hindlimb ischemia model. Our results extend these early observations, wherein we report increased β-catenin expression and enhanced Wnt gene expression in the cerebral vessels at 1 and 7 days after TBI. Together, our findings suggest that Wnt/β-catenin expression likely has a role in vascular repair and represents a potential target for future therapeutics for TBI and other brain injuries.

Numerous angiogenic factors are up-regulated after TBI and have distinct expression profiles and functions. One such molecule is VEGF, which plays a role in post-stroke angiogenesis.[56] Experimental studies using animal models of TBI have reported up-regulation in VEGF expression at 3–7 dpi.[9,57,58] An important finding was the rapid up-regulation of β-catenin in the cortical vessels, indicating that β-catenin may be the driving force for vascular repair by regulating the expression of VEGF and other putative angiogenic factors. The VEGF promoter contains seven binding sites for β-catenin/TCF,[59] and β-catenin has been shown to increase VEGF expression after hindlimb ischemic injury.[17] Thus, β-catenin may directly regulate VEGF expression or act in parallel with VEGF to promote vascular repair after TBI.

In summary, the cerebral vasculature participates in the pathogenesis of TBI and treatments that can enhance vascular repair and restore vascular function are critical for functional outcome. This study provides quantitative morphometric information on the vascular network in acute and subacute stages of TBI. The Wnt/β-catenin signaling pathway has been studied in the context of regeneration, neuronal, and glial cell populations, after TBI.[20,22,23] The present study is the first to examine this pathway in the context of vascular repair after TBI. We are the first to report increased β-catenin expression and activation of Wnt genes in the vasculature early after TBI, suggesting that Wnt/β-catenin signaling may be a key player in the initiation of vascular repair. Our results open up the possibility of targeting the Wnt/β-catenin signaling pathway to enhance vascular repair as a therapeutic target for TBI. The Wnt/β-catenin signaling pathway may work in conjunction with Notch signaling to activate vascular repair genes after injury. Ongoing research will be needed to discover the molecular mechanisms underlying Wnt/β-catenin-mediated vascular repair.

Resource sharing

We will provide published data and relevant protocols upon request. Unpublished information can be made available by providing a request to the Principal Investigator by phone call or email.

Funding

The author(s) disclosed receipt of the following financial support for the research, authorship, and/or publication of this article: NIH Program Project grant from National Institute of Neurological Disorders and Stroke (1P01NS082184, Project 3).

Acknowledgements

The authors also thank Anastasia Ibrahim for help in optimizing the immunohistochemistry protocol.

Declaration of conflicting interests

The author(s) declared no potential conflicts of interest with respect to the research, authorship, and/or publication of this article.

Authors' contributions

AS, AJ, MH, VD, and AO contributed to conception and design of the study. AS, AJ, MB, MW, and VD acquired and analyzed the data. AS, AJ, and AO drafted a significant portion of the manuscript or figures. JT, JHZ, and WJP analyzed the data and edited the final draft. All authors read and approved the final version of the manuscript.

Supplementary material

Supplementary material for this paper can be found at the journal website: http://journals.sagepub.com/home/jcb

References

1. Jullienne A, Obenaus A, Ichkova A, et al. Chronic cerebrovascular dysfunction after traumatic brain injury. *J Neurosci Res* 2016; 94: 609–622.
2. Salehi A, Zhang JH and Obenaus A. Response of the cerebral vasculature following traumatic brain injury. *J Cereb Blood Flow Metab* 2017; 37: 2320–2339.
3. Soustiel JF, Glenn TC, Shik V, Boscardin J, et al. Monitoring of cerebral blood flow and metabolism in traumatic brain injury. *J Neurotrauma* 2005; 22: 955–965.
4. Adams JH, Jennett B, Murray LS, et al. Neuropathological findings in disabled survivors of a head injury. *J Neurotrauma* 2011; 28: 701–709.
5. Park E, Bell JD, Siddiq IP, et al. An analysis of regional microvascular loss and recovery following two grades of fluid percussion trauma: a role for hypoxia-inducible factors in traumatic brain injury. *J Cereb Blood Flow Metab* 2009; 29: 575–584.
6. Siddiq I, Park E, Liu E, et al. Treatment of traumatic brain injury using zinc-finger protein gene therapy targeting VEGF-A. *J Neurotrauma* 2012; 29: 2647–2659.
7. Hayward NM, Tuunanen PI, Immonen R, et al. Magnetic resonance imaging of regional hemodynamic and cerebrovascular recovery after lateral fluid-percussion brain injury in rats. *J Cereb Blood Flow Metab* 2011; 31: 166–177.
8. Krum JM and Khaibullina A. Inhibition of endogenous VEGF impedes revascularization and astroglial proliferation: roles for VEGF in brain repair. *Exp Neurol* 2003; 181: 241–257.
9. Skold MK, von Gertten C, Sandberg-Nordqvist AC, et al. VEGF and VEGF receptor expression after experimental brain contusion in rat. *J Neurotrauma* 2005; 22: 353–367.
10. Zhang ZG, Zhang L, Jiang Q, et al. VEGF enhances angiogenesis and promotes blood-brain barrier leakage in the ischemic brain. *J Clin Invest* 2000; 106: 829–838.
11. Corada M, Morini MF and Dejana E. Signaling pathways in the specification of arteries and veins. *Arterioscler Thromb Vasc Biol* 2014; 34: 2372–2377.
12. Birdsey GM, Shah AV, Dufton N, et al. The endothelial transcription factor ERG promotes vascular stability and growth through Wnt/beta-catenin signaling. *Dev Cell* 2015; 32: 82–96.
13. Corada M, Nyqvist D, Orsenigo F, et al. The Wnt/beta-catenin pathway modulates vascular remodeling and specification by upregulating Dll4/Notch signaling. *Dev Cell* 2010; 18: 938–949.
14. Zhou Y, Wang Y, Tischfield M, et al. Canonical WNT signaling components in vascular development and barrier formation. *J Clin Invest* 2014; 124: 3825–3846.
15. Daneman R, Agalliu D, Zhou L, et al. Wnt/beta-catenin signaling is required for CNS, but not non-CNS, angiogenesis. *Proc Natl Acad Sci USA* 2009; 106: 641–646.

16. Wang X, Xiao Y, Mou Y, et al. A role for the beta-catenin/T-cell factor signaling cascade in vascular remodeling. *Circ Res* 2002; 90: 340–347.
17. Kim KI, Cho HJ, Hahn JY, et al. Beta-catenin overexpression augments angiogenesis and skeletal muscle regeneration through dual mechanism of vascular endothelial growth factor-mediated endothelial cell proliferation and progenitor cell mobilization. *Arterioscler Thromb Vasc Biol* 2006; 26: 91–98.
18. Lambert C, Cisternas P and Inestrosa NC. Role of Wnt signaling in central nervous system injury. *Mol Neurobiol* 2016; 53: 2297–2311.
19. Shapira M, Licht A, Milman A, et al. Role of glycogen synthase kinase-3beta in early depressive behavior induced by mild traumatic brain injury. *Mol Cell Neurosci* 2007; 34: 571–577.
20. Wu X, Mao H, Liu J, et al. Dynamic change of SGK expression and its role in neuron apoptosis after traumatic brain injury. *Int J Clin Exp Pathol* 2013; 6: 1282–1293.
21. Zhang YM, Dai QF, Chen WH, et al. Effects of acupuncture on cortical expression of Wnt3a, beta-catenin and Sox2 in a rat model of traumatic brain injury. *Acupunct Med* 2016; 34: 48–54.
22. White BD, Nathe RJ, Maris DO, et al. Beta-catenin signaling increases in proliferating NG2+ progenitors and astrocytes during post-traumatic gliogenesis in the adult brain. *Stem Cells* 2010; 28: 297–307.
23. Zhang L, Yan R, Zhang Q, et al. Survivin, a key component of the Wnt/beta-catenin signaling pathway, contributes to traumatic brain injury-induced adult neurogenesis in the mouse dentate gyrus. *Int J Mol Med* 2013; 32: 867–875.
24. Donovan V, Bianchi A, Hartman R, et al. Computational analysis reveals increased blood deposition following repeated mild traumatic brain injury. *Neuroimage Clin* 2012; 1: 18–28.
25. Obenaus A, Ng M, Orantes AM, et al. Traumatic brain injury results in acute rarefication of the vascular network. *Sci Rep* 2017; 7: 1–14.
26. Zudaire E, Gambardella L, Kurcz C, et al. A computational tool for quantitative analysis of vascular networks. *PLoS One* 2011; 6: e27385.
27. Cole JT, Yarnell A, Kean WS, et al. Craniotomy: true sham for traumatic brain injury, or a sham of a sham? *J Neurotrauma* 2011; 28: 359–369.
28. Obenaus A, Ng M, Orantes A, et al. Traumatic brain injury results in acute rarefication of the vascular network. *Sci Rep* 2017; 7: 239.
29. Walchli T, Mateos JM, Weinman O, et al. Quantitative assessment of angiogenesis, perfused blood vessels and endothelial tip cells in the postnatal mouse brain. *Nat Protoc* 2015; 10: 53–74.
30. Grumolato L, Liu G, Mong P, et al. Canonical and noncanonical Wnts use a common mechanism to activate completely unrelated coreceptors. *Genes Dev* 2010; 24: 2517–2530.
31. Zanetta L, Marcus SG, Vasile J, et al. Expression of Von Willebrand factor, an endothelial cell marker, is up-regulated by angiogenesis factors: a potential method for objective assessment of tumor angiogenesis. *Int J Cancer* 2000; 85: 281–288.
32. Sakata N, Chan NK, Chrisler J, et al. Bone marrow cell cotransplantation with islets improves their vascularization and function. *Transplantation* 2010; 89: 686–693.
33. Corada M, Orsenigo F, Morini MF, et al. Sox17 is indispensable for acquisition and maintenance of arterial identity. *Nat Commun* 2013; 4: 1–14.
34. Gama Sosa MA, De Gasperi R, Janssen PL, et al. Selective vulnerability of the cerebral vasculature to blast injury in a rat model of mild traumatic brain injury. *Acta Neuropathol Commun* 2014; 2: 1–18.
35. Lange C, Turrero Garcia M, Decimo I, et al. Relief of hypoxia by angiogenesis promotes neural stem cell differentiation by targeting glycolysis. *EMBO J* 2016; 35: 924–941.
36. Gong D, Zhang S, Liu L, et al. Dynamic changes of vascular endothelial growth factor and angiopoietin-1 in association with circulating endothelial progenitor cells after severe traumatic brain injury. *J Trauma* 2011; 70: 1480–1484.
37. Gong D, Hao M, Liu L, et al. Prognostic relevance of circulating endothelial progenitor cells for severe traumatic brain injury. *Brain Injury* 2012; 26: 291–297.
38. Veenith TV, Carter EL, Geeraerts T, et al. Pathophysiologic mechanisms of cerebral ischemia and diffusion hypoxia in traumatic brain injury. *JAMA Neurol* 2016; 73: 542–550.
39. Xu K and Lamanna JC. Chronic hypoxia and the cerebral circulation. *J Appl Physiol* 2006; 100: 725–730.
40. Ward NL, Moore E, Noon K, et al. Cerebral angiogenic factors, angiogenesis, and physiological response to chronic hypoxia differ among four commonly used mouse strains. *J Appl Physiol* 2007; 102: 1927–1935.
41. Robertson RT, Levine ST, Haynes SM, et al. Use of labeled tomato lectin for imaging vasculature structures. *Histochem Cell Biol* 2015; 143: 225–234.
42. Hughes S, Dashkin O and Defazio RA. Vessel painting technique for visualizing the cerebral vascular architecture of the mouse. *Meth Mol Biol* 2014; 1135: 127–138.
43. Carmeliet P and Jain RK. Molecular mechanisms and clinical applications of angiogenesis. *Nature* 2011; 473: 298–307.
44. Oertel M, Boscardin WJ, Obrist WD, et al. Posttraumatic vasospasm: the epidemiology, severity, and time course of an underestimated phenomenon: a prospective study performed in 299 patients. *J Neurosurg* 2005; 103: 812–824.
45. Alford PW, Dabiri BE, Goss JA, et al. Blast-induced phenotypic switching in cerebral vasospasm. *Proc Natl Acad Sci USA* 2011; 108: 12705–12710.
46. Schwarzmaier SM, Kim SW, Trabold R, et al. Temporal profile of thrombogenesis in the cerebral microcirculation after traumatic brain injury in mice. *J Neurotrauma* 2010; 27: 121–130.
47. Lu D, Mahmood A, Goussev A, et al. Delayed thrombosis after traumatic brain injury in rats. *J Neurotrauma* 2004; 21: 1756–1766.

48. Goentoro L and Kirschner MW. Evidence that fold-change, and not absolute level, of beta-catenin dictates Wnt signaling. *Mol Cell* 2009; 36: 872–884.
49. Nusse R and Clevers H. Wnt/beta-catenin signaling, disease, and emerging therapeutic modalities. *Cell* 2017; 169: 985–999.
50. Topol L, Jiang X, Choi H, et al. Wnt-5a inhibits the canonical Wnt pathway by promoting GSK-3-independent beta-catenin degradation. *J Cell Biol* 2003; 162: 899–908.
51. Bernard P, Fleming A, Lacombe A, et al. Wnt4 inhibits beta-catenin/TCF signalling by redirecting beta-catenin to the cell membrane. *Biol Cell* 2008; 100: 167–177.
52. Liebner S, Corada M, Bangsow T, et al. Wnt/beta-catenin signaling controls development of the blood-brain barrier. *J Cell Biol* 2008; 183: 409–417.
53. Stenman JM, Rajagopal J, Carroll TJ, et al. Canonical Wnt signaling regulates organ-specific assembly and differentiation of CNS vasculature. *Science* 2008; 322: 1247–1250.
54. Lengfeld JE, Lutz SE, Smith JR, et al. Endothelial Wnt/beta-catenin signaling reduces immune cell infiltration in multiple sclerosis. *Proc Natl Acad Sci USA* 2017; 114: E1168–E1177.
55. Lim RG, Quan C, Reyes-Ortiz AM, et al. Huntington's disease iPSC-derived brain microvascular endothelial cells reveal WNT-mediated angiogenic and blood-brain barrier deficits. *Cell Rep* 2017; 19: 1365–1377.
56. Lennmyr F, Ata KA, Funa K, et al. Expression of vascular endothelial growth factor (VEGF) and its receptors (Flt-1 and Flk-1) following permanent and transient occlusion of the middle cerebral artery in the rat. *J Neuropathol Exp Neurol* 1998; 57: 874–882.
57. Nag S, Takahashi JL and Kilty DW. Role of vascular endothelial growth factor in blood-brain barrier breakdown and angiogenesis in brain trauma. *J Neuropathol Exp Neurol* 1997; 56: 912–921.
58. Papavassiliou E, Gogate N, Proescholdt M, et al. Vascular endothelial growth factor (vascular permeability factor) expression in injured rat brain. *J Neurosci Res* 1997; 49: 451–460.
59. Easwaran V, Lee SH, Inge L, et al. beta-Catenin regulates vascular endothelial growth factor expression in colon cancer. *Cancer Res* 2003; 63: 3145–3153.